A&A 676, C2 (2023)
https://doi.org/10.1051/0004-6361/202244547e

Astronomy & Astrophysics

LETTER TO THE EDITOR

GBT/MUSTANG-2 900 resolution imaging of the SZ effect in MS0735.6+7421

Confirmation of the SZ cavities through direct imaging *(Corrigendum)*

John Orlowski-Scherer[1], Saianeesh K. Haridas[1], Luca Di Mascolo[2,3,4], Karen Perez Sarmiento[1], Charles E. Romero[5], Simon Dicker[1], Tony Mroczkowski[6], Tanay Bhandarkar[1], Eugene Churazov[7,8], Tracy E. Clarke[9], Mark Devlin[1], Massimo Gaspari[10], Ian Lowe[11], Brian Mason[12], Craig L. Sarazin[13], Jonathon Sievers[14], and Rashid Sunyaev[7,8]

[1] Department of Physics and Astronomy, University of Pennsylvania, 209 South 33rd Street, Philadelphia, PA 19104, USA
e-mail: jorlo@sas.upenn.edu
[2] Department of Physics, University of Trieste, via Tiepolo 11, 34131 Trieste, Italy
[3] INAF–Osservatorio Astronomico di Trieste, via Tiepolo 11, 34131 Trieste, Italy
[4] IFPU–Institute for Fundamental Physics of the Universe, via Beirut 2, 34014 Trieste, Italy
[5] Center for Astrophysics | Harvard and Smithsonian, 60 Garden Street, Cambridge, MA 02143, USA
[6] European Southern Observatory (ESO), Karl-Schwarzschild-Strasse 2, 85741 Garching, Germany
[7] Max Planck Institute for Astrophysics, Karl-Schwarzschild-Strasse 1, 85741 Garching, Germany
[8] Space Research Institute (IKI), Profsoyuznaya 84/32, Moscow 117997, Russia
[9] Naval Research Laboratory, Code 7213, 4555 Overlook Ave SW, Washington, DC 20375, USA
[10] Department of Astrophysical Sciences, Princeton University, Princeton, NJ 08544, USA
[11] Department of Astronomy, University of Arizona, Tucson, AZ 85721, USA
[12] NRAO, 520 Edgemont Rd, Charlottesville, VA 22903, USA
[13] Department of Astronomy, University of Virginia, 530 McCormick Road, Charlottesville, VA 22904-4325, USA
[14] Department of Physics, McGill University, 3600 University Street, Montreal, QC H3A 2T8, Canada

A&A 667, L6 (2022), https://doi.org/10.1051/0004-6361/202244547

Key words. galaxies: clusters: individual: MS0735.6+7421 – galaxies: clusters: intracluster medium – cosmic background radiation – errata, addenda

In the course of refactoring the code used to perform model fitting in Orlowski-Scherer et al. (2022), it was discovered that the beam size used was incorrect. MUSTANG-2 uses two concentric Gaussian beam profiles to represent the inner beam and the extended wings (e.g. Romero et al. 2020). For each of the Gaussians, the amplitude of the Gaussian and its full width at half maximum had been swapped. This resulted in incorrect smoothing of the map. We have completely rerun the analysis using the more accurate beam. There are no significant changes to our results. In general, the suppression factors, f, increase by about 1σ from the values quoted in Orlowski-Scherer et al. (2022), but remain consistent with either non-thermal pressure support or a mixture of extremely hot thermal and non-thermal support. In fact, our results are less consistent with purely thermal support, although we still cannot completely rule out pure thermal support. Additionally, we no longer find statistically significant support for an outer profile slope, β_1, which differs from the X-ray-inferred value from Vantyghem et al. (2014) when not performing time ordered data (TOD) subtraction; this is a very minor change. In this erratum we include updated versions of all the tables and plots that were affected by this bug.

In general, using this improved representation of the MUSTANG-2 beam has not changed the results of

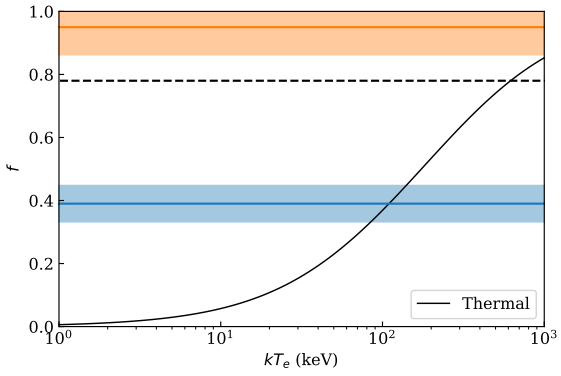

Fig. 1. Updated plot of the suppression factor, f, vs. kT for the thermal support case. This is an updated version of Fig. 2 in the original paper, with the values of f updated; the theory curves are the same. $f = 1$ means complete suppression, i.e., no SZ signal from the bubbles, while $f = 0$ means no suppression, i.e., the signal within the bubble is identical to the global ICM signal. The blue band shows the best-fit f with 1σ uncertainties for the lowest f case considered, corresponding to thermal pressure support by electrons with temperatures of at least 110 keV. The dashed line shows the lowest value consistent with Abdulla et al. (2019) to 1σ.

Table 1. Updated summary of the results of the various fitting routines we completed.

TOD Subtract	β_1	$\mathcal{M}$	r_3	f_{NE}	f_{SW}	T_{NE} (keV)	T_{SW} (keV)	Significance
Yes	1.29 ± 0.06	0	r_1	0.95 ± 0.09	0.74 ± 0.10	3100^{+3000}_{-1000}	500^{+900}_{-100}	8.31
Yes	1.32 ± 0.06	0	r_2	0.73 ± 0.07	0.57 ± 0.08	475^{+225}_{-175}	250^{+100}_{-50}	8.35
No	0.97 ± 0.04	0	r_1	0.79 ± 0.08	0.51 ± 0.08	650^{+500}_{-225}	175^{+75}_{-50}	8.43
No	1.10 ± 0.04	0	r_2	0.61 ± 0.06	0.40 ± 0.06	275^{+75}_{-75}	115^{+30}_{-25}	8.17
Yes	0.98	0	r_1	0.81 ± 0.09	0.60 ± 0.10	750^{+800}_{-300}	400^{+250}_{-150}	7.12
Yes	0.98	0	r_2	0.62 ± 0.07	0.46 ± 0.08	275^{+100}_{-75}	150^{+50}_{-50}	7.02
No	0.98	0	r_1	0.80 ± 0.07	0.52 ± 0.08	700^{+450}_{-225}	200^{+75}_{-50}	8.52
No	0.98	0	r_2	0.61 ± 0.06	0.39 ± 0.06	275^{+75}_{-75}	110^{+30}_{-25}	8.41
Yes	0.98	1.78 ± 0.14	r_1	0.93 ± 0.09	0.71 ± 0.10	2250^{+3000}_{-1325}	425^{+300}_{-150}	8.49
Yes	0.98	1.82 ± 0.14	r_2	0.77 ± 0.07	0.61 ± 0.08	575^{+325}_{-175}	275^{+75}_{-75}	8.61
No	0.98	1.15 ± 0.05	r_1	0.84 ± 0.07	0.55 ± 0.08	900^{+800}_{-325}	225^{+75}_{-50}	8.90
No	0.98	1.20 ± 0.05	r_2	0.67 ± 0.06	0.45 ± 0.06	350^{+150}_{-100}	140^{+40}_{-30}	8.99

Notes. This table is the equivalent of Table 3 in the original paper, with all of the values for β_1, $\mathcal{M}$, f_{NE}, f_{SW}, T_{NE}, T_{SW}, and the significances updated. "TOD subtract" indicates whether the estimated elevation synchronous signal was subtracted from the data or not. β_1 is the power law for the outer beta profile: if no uncertainty is given, then it was fixed in that model; if an uncertainty is given, then it was a free parameter. $\mathcal{M}$ is the Mach number; if it is 0, then the shock was not included in that fit. The column r_3 indicates whether the line-of-sight core radius was set to the semimajor (r_1) or semiminor (r_2) core radius. f_{NE} and f_{SW} are the suppression factors for the northeast and southwest bubbles, respectively. T_{NE} and T_{SW} are the implied temperatures in the bubbles assuming full pressure support; it is the temperature implied by f as shown in Fig. 1. For each model, an F-test was performed between that model and the same model without cavities. The significance of this test is reported in the last column.

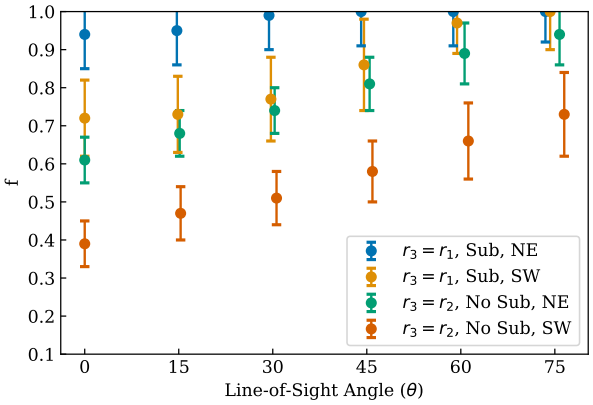

Fig. 2. Updated plot of the suppression factor, f, as a function of the line-of-sight angle, with $\theta = 0$ being in the plane of the sky and $\theta = 90$ lying along the z-axis. This is an updated version of Fig. 3 from the original paper, with updated values for f. Shown is the f for both the northeast and southwest cavities for the scenarios in Table 1 that include shocks with the highest and lowest suppression factors. Explicitly, they are: with shock, $r_3 = r_1$, and with TOD subtraction; and with shock, $r_3 = r_2$, and without TOD subtraction. In general, f increases with increasing θ, although we do not completely lose our ability to distinguish between pressure support scenarios, e.g., we can still rule out $f = 1$ for the southwest cavity in the $r_3 = r_2$ without TOD subtraction.

Orlowski-Scherer et al. (2022). The exact suppression factors have changed slightly, however, and as such we report them here. These new suppression factors should be used instead of those found in Orlowski-Scherer et al. (2022).

Table 2. Updated statistical significance of the improvement of fit as determined by an F-test for freeing the outer slope, β_1, for various combinations of TOD subtraction and r_3 values. This is the equivalent of Table 4 in the original Letter. Values for β_1 and the significance of detection have been updated here. This includes the only substantive update from this erratum; the detections without TOD subtraction are no longer statistically significant. In general, the fit is improved at a statistically significant level when performing TOD subtraction, but did not improve without it. This is indicative of a degeneracy between the bowling of the maps and β_1.

TOD Subtract	β_1	r_3	Significance
Yes	1.29 ± 0.06	r_1	7.06
Yes	1.32 ± 0.06	r_2	8.00
No	0.97 ± 0.04	r_1	0
No	1.10 ± 0.04	r_2	0

Table 3. Updated statistical significance of the improvement of fit as determined by an F-test for adding the shock enhancement for various combinations of TOD subtraction and r_3 values. This is an updated version of Table 5 of the original work. Values of $\mathcal{M}$ and their significances have been updated. The inclusion is very statistically significant when TOD subtraction is performed, but marginal when it is not. This may be because the bowling is of comparable scale to the shock, and hence without TOD subtraction we have difficulty detecting the shock.

TOD Subtract	$\mathcal{M}$	r_3	Significance
Yes	1.78 ± 0.14	r_1	9.91
Yes	1.82 ± 0.14	r_2	11.40
No	1.15 ± 0.05	r_1	3.60
No	1.20 ± 0.05	r_2	5.32

References

Abdulla, Z., Carlstrom, J. E., Mantz, A. B., et al. 2019, ApJ, 871, 195
Orlowski-Scherer, J., Haridas, S. K., Di Mascolo, L., et al. 2022, A&A, 667, L6
Romero, C. E., Sievers, J., Ghirardini, V., et al. 2020, ApJ, 891, 90
Vantyghem, A. N., McNamara, B. R., Russell, H. R., et al. 2014, MNRAS, 442, 3192